A review of the Limerick Igneous Suite: links to base-metal mineralization in the SW Irish Orefield

Paul Slezak[1], Danny Hnatyshin[1,2], Alejandro Andrés[3], Eoin Dunlevy[4], Hilde Koch[5], Mark Holdstock[6], & Murray W. Hitzman[1]

[1] Irish Centre for Research in Applied Geosciences (iCRAG), UCD School of Earth Sciences, University College Dublin, Dublin 4, Ireland

[2] Natural Resources Canada, Geological Survey of Canada, 601 Booth Street, Ottawa, Ontario K1A0EA, Canada

[3]Laboratory of Planetology and Geosciences, STU Department of the Faculty of Sciences and Techniques, Nantes Université, 2 Chem. de la Houssinière Bâtiment 4, 44300 Nantes, France

[4]Terranta GmbH, Rathausstraße 37a | 52072 Aachen, Germany

[5]Earth Surface Research Laboratory (ESRL), Unit 6b, Trinity Technology & Enterprise Centre (TTEC), Pearce Street, Dublin 2, Ireland

[6] Group Eleven Mining & Exploration Ltd, 22 Northumberland Road, Dublin 4, Ireland

Abstract: The Limerick Igneous Suite (LIS) in SW Ireland consists of massive flows, hypabyssal intrusions, tuffs, agglomerates, and diatremes and is spatially associated with multiple base metal prospects, deposits, and historic mines in the Limerick Syncline. The LIS is subdivided into two igneous units: 1) the Knockroe, which is dominantly alkaline basalt to trachyandesite in composition, and 2) the Knockseefin, which forms a range of alkaline basalt to basanite compositions. Recent drilling has uncovered new, olivine-bearing porphyritic basalts that correspond to the Knockroe unit and may represent the highest degree of partial melting in the LIS. A new sulphide Re–Os isochron from the Ballywire prospect yielded an age of 340.9 ± 2.4 Ma and represents the first known mineralization age in the Limerick Syncline, which is contemporaneous with LIS emplacement. However, the $^{187}Os/^{188}Os$ of 0.48 is indicative of base metal derivation from crustal rocks akin to Palaeozoic basement as opposed to an igneous or mafic source. The LIS was not likely a source of metals, but the coeval emplacement between the LIS and mineralization in the Limerick Syncline suggests the LIS may have been a source of hydrothermalism in the region. Yet the intrusions themselves were emplaced in fault networks, hindering rather than enhancing hydrothermal fluid flow.

Keywords: Re–Os dating, base metals, Limerick Igneous Suite, basalt, basanite, Ballywire age dating.

Introduction

The Irish Orefield contains a number of significant base metal deposits hosted in Carboniferous limestones. The deposits formed from deeply circulating, moderate temperature brines that transported metals along deep-seated, basin-wide faults (Hitzman & Beaty, 1996; Hitzman *et al*., 2002; Wilkinson *et al.*, 2005a, 2005b; Ashton *et al*., this volume). Most of the known Irish-type deposits are not typically associated with significant igneous activity. However, in the Limerick Syncline (Co. Limerick, Ireland) multiple base metal deposits and prospects occur spatially with a variety of mafic igneous units, which comprise the Limerick Igneous Suite (LIS). Determining the influence of igneous activity on base metal mineralization is crucial in refining both local and regional models for Irish-type mineralization.

The LIS is composed of two geochemically distinct, but relatively continuous, units: the Knockroe and Knockseefin igneous units (Strogen, 1983;1988; Elliott *et al.*, 2015; Slezak *et al*., 2023). These units intrude the lower Carboniferous sedimentary package, which fills the Limerick Syncline and is the typical host for base metal deposits. Biostratigraphy constrains these igneous units to the Viséan (347 – 331 Ma; Somerville *et al*.; 1992) with more recent U–Pb dates on igneous apatite showing the igneous units were emplaced *c.* 353 ± 6 Ma (Slezak *et al*., 2023). Slezak *et al.* (2023) also calculated alteration ages of the igneous rocks using Rb–Sr bulk rock isotope data, which correlate to the older U–Pb, and younger biostratigraphic dates. These ages broadly agree with pyrite Re–Os ages of 347 ± 3 Ma and 334 ± 6 Ma from Lisheen and Silvermines, respectively, (Hnatyshin *et al*., 2015) as well as a recent 331 ± 6 Ma U–Pb date from hydrothermal apatite in hydrothermal dolostone at Silvermines (Vafeas *et al*., 2023).

Previous workers (McCusker & Reed, 2013; Elliot *et al*., 2019)

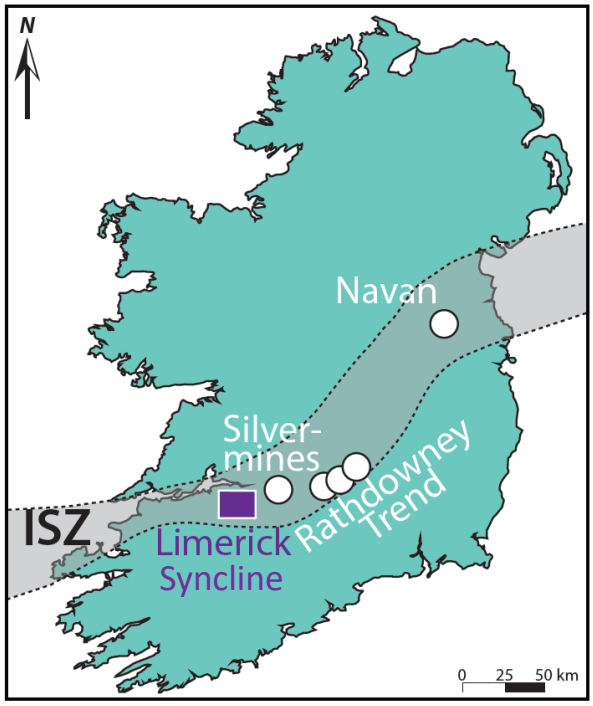

Figure 1: *Overview of major Irish-type deposit locations in relation to the full potential extent of Iapetus Suture Zone (ISZ) as depicted from Ashton et al. (this volume).*

have suggested the LIS facilitated mineralization by creating fracture networks and fluid pathways during emplacement in lieu of the major basin-bounding faults typically associated with Irish-type deposits (Hitzman & Beaty, 1996). In addition, several studies (e.g., Kerr, 2013 and Elliot *et al*., 2019) reported $\delta^{34}S$ isotope values ranging from -42 ‰ to +13 ‰, suggesting a mixed affinity between biogenically reduced sulphate and potential igneous sulphur sources, attributing the more positive $\delta^{34}S$ values with igneous reservoirs (Sakai *et al*., 1984; Seal, 2006).

However, most Irish-type deposits display a wide range of $\delta^{34}S$ values (e.g., Wilkinson & Hitzman, 2015), suggesting that the sulphur isotopic data in the Limerick deposits is not indicative of a purely igneous source. In this study, we review the LIS, provide new geochemical data on recently discovered olivine-bearing units in addition to extrusive units, and present a new Re–Os isochron from the Ballywire prospect (see Fig. 2 for location), which establishes the first base metal mineralization age in the Limerick Syncline.

Furthermore, we assess isotope sources using Os isotopes from this study and Nd and Sr isotopes (from Slezak *et al*., 2023; Cordiero *et al.*, 2023) to evaluate whether the LIS could have been a metal source. The crustal Os ratios compared to the mantle-like Nd and Sr ratios indicate that rather than being a source of base metals, the LIS was not a source of base metals but rather likely a heat source that facilitated hydrothermal fluid circulation.

Geologic Background

Limerick Igneous Suite rocks crop out in and around the Limerick Syncline, a subbasin along the multi-kilometre wide Iapetus Suture Zone (ISZ; Figs. 1 and 2). Most Irish-type base metal deposits and prospects occur along the ISZ (Fig. 1), which joins together Ganderia-Avalonia in the southeast and Laurentia in the northwest of Ireland (Vaughan & Johnston, 1992; Chew & Stillman, 2009; McConnell *et al*., 2021; Ashton *et al,* this volume).

Limerick Syncline stratigraphy

The Limerick Syncline comprises a transgressive succession of Tournasian to Viséan (i.e., early to late Mississippian) limestones and alkaline basaltic igneous units (Fig. 2) that sit conformably atop or intrude the sub-aerial, siliciclastic units of the Devonian Old Red Sandstone (Graham, 2009; Sevastopulo & Wyse-Jackson, 2009). Above the Old Red Sandstone lies the Lower Limestone Shale Formation, which records a shift from sub-aerial to marine conditions and comprises interbedded sandstones, shales and calcarenites showing an upward increase in bioclastic and carbonate content, reflecting establishment of progressively more open marine conditions. The overlying Ballysteen Formation is a package of argillaceous bioclastic limestones and biosparites rich in crinoid debris that record an overall deepening upward trend with the upper-most portions deposited below storm wave base (Sevastopulo & Wyse-Jackson, 2009). In the Limerick Syncline, the Ballysteen Group is succeeded by the Waulsortian Limestone Formation, which is dominated by pale grey, stromatactis-bearing micrites/biomicrites that likely were deposited as biogenic mud-mounds below storm wave base but within the photic zone (Strogen & Somerville, 1984; Strogen, 1988; Devuyst & Lees, 2001). The Lough Gur Formation sits atop the Waulsortian Limestone Formation (Fig. 2) and is composed of fossiliferous, crinoid-rich wackestones and packestones with zones of abundant chert (Strogen, 1988; Somerville *et al*., 1992). The unit is generally lithologically and sedimentologically similar to limestones within the Ballysteen Formation. The Knockroe igneous unit comprises an alkaline basaltic suite that has an intercalated basal contact (often erosive) with the Lough Gur Formation (Fig. 2). The Herbertstown Limestone Formation interfingers with the Knockroe rocks below and the Knockseefin igneous unit above. It consists mostly of beige to pale blue oolitic grainstones, packestones, and micrites with solitary corals deposited in a shallow water environment (Strogen, 1988; Somerville et al., 1992). The overlying Knockseefin igneous unit is comprised of alkaline basaltic to basanitic rocks. However, in some areas in the central portion of the Limerick Syncline (see Fig. 2), the Knockroe directly transitions to Knockseefin rocks over a 10m interval of volcaniclastic material. The Dromkeen Limestone Formation is the uppermost carbonate unit preserved in the area (Fig. 2) and is comprised of shallow water, fine-grained grainstones that contain several palaeosol horizons indicating a shallow depositional environment and either sea level changes or tectonic uplift (Somerville *et al*., 2011). The sedimentary succession was then partially eroded and is capped by an unconformity overlain by Namurian siliciclastic shales, silts, and sands of the Longstone Formation (Strogen, 1988).

Limerick Igneous Suite (LIS)

The LIS is made up of two igneous units: 1) the Knockroe and, 2) the Knockseefin (see Figure 2). The Knockroe unit is

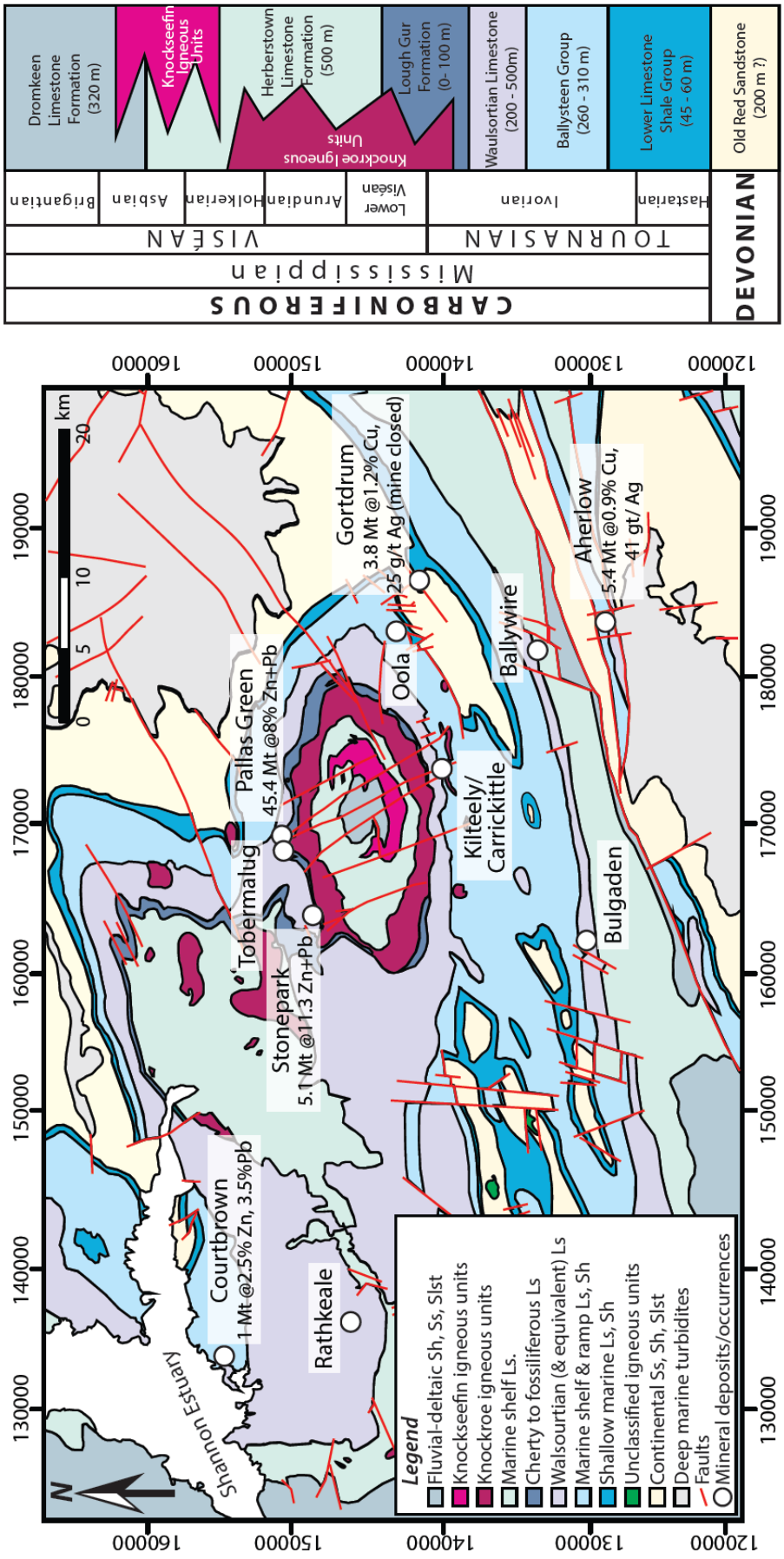

Figure 2.: *Base-metal deposits and occurrence locations and idealised stratigraphy in the Limerick Syncline. (Modified from Figures 1 and 2 from Slezak et al. (2023), used under CC-BY-4.0).*

dominated by alkaline basaltic to trachytic composition volcanic rocks comprised of a series of early basaltic maar-diatremes and volcanic tuffs, the eruption of which were followed by emplacement of hypabyssal intrusions, submarine flows, agglomerates, igneous breccias, tuffs, and volcaniclastic units (Strogen, 1983; 1988; Elliott *et al.*, 2015). These rocks are occasionally interbedded with limestones and shale. They are also occasionally crosscut by slightly later, but chemically similar porphyritic alkaline basalt dykes (Slezak *et al*., 2023).

Knockroe unit

Diatremes

The diatremes are heterolithic and often light grey-green to light beige in colour, though these rocks readily oxidise on exposure to the atmosphere taking on a rust-colour in many examples. The diatremes consist of clasts of vesicular basalt, agglomerates, tuffs, and xenoliths of dominantly carbonate wall rock set in a fine-grained, ashy matrix (Fig. 3a). The xenoliths are predominantly Waulsortian Limestone (Fig. 3a) but in some bodies clasts of underlying units including Old Red Sandstone and basement rocks are found. Basement xenoliths include amphibolite-grade metasedimentary rocks, mafic granulite, and tonalitic orthogneiss (van den Berg *et al*., 2005; O'Rourke, 2013). Clasts are variable in size and have been described by Elliott et al. (2015), who established eight lithofacies and five lithofacies associations for the diatremes. Strong clay, chlorite, and carbonate alteration is ubiquitous in the diatremes, but some fresher basalt clasts are occasionally present (Fig. 3a). They may also contain minor to moderate amounts of generally disseminated pyrite.

Lava flows and intrusive units

The Knockroe unit contains massive seafloor flows consisting of dark grey to green blue and greyish green to maroon-coloured rocks with aphanitic to porphyritic textures (Fig. 3b). Some flows exhibit as a flow top crackle to jigsaw breccia in a carbonate matrix. The Knockroe unit also contains relatively abundant igneous breccias containing basaltic clasts in a basaltic matrix (Fig. 3b). Knockroe intrusive units are typically hypabyssal intrusions as dikes and less commonly sills.

For the units found in the centre of the Limerick Syncline (Fig. 2), plagioclase is the most common mineral in these units and occurs as euhedral laths that dominate the phenocrystic and matrix phases (Fig. 3b and Fig. 4a). Minor amounts of potassium feldspar are also present as rare anhedral phenocrysts and more often mantling plagioclase crystals in the matrix (Slezak *et al*., 2023). Clinopyroxene, likely augite and commonly altered, is less abundant than plagioclase. It is typically euhedral, phenocrystic, and may be zoned and/or contain inclusions of magnetite. Magnetite is present mainly in the matrix as small, anhedral to subhedral crystals (Fig. 4a), though it can present as larger phenocrysts. Apatite is present in trace amounts as small, ovoid crystals (Slezak *et al*., 2023). Subhedral, rounded phenocrysts of olivine may have been present in many samples. Where present, it has generally been altered to magnetite/haematite, calcite, chlorite, and rare serpentinite (Fig. 4b).

Recently, relatively fresh, porphyritic olivine basalts (Fig. 3c) have been found in Group Eleven drillhole GC-2654-1, near Ballywire, Co. Tipperary (Fig. 2), which are geochemically similar the Knockroe units (see below). This subset of the Knockroe units contains higher abundances (~15-20 %) of subhedral to euhedral phenocrystic olivine (up to 2300μm) with larger grains displaying serpentinized rims and smaller grains being wholly replaced (Fig. 4c). Clinopyroxene is also phenocrystic, up to 3400 μm in size, often twinned and/or zoned (Fig. 4b), and more abundant (~30%) compared to the Knockroe units reported by Slezak *et al*. (2023). Plagioclase is zoned and present as both a phenocrystic phase (up to 1500 μm) and the predominant matrix phase (~100 – 200 μm). Magnetite is also present as smaller (20 - 100 μm), subhedral crystals in the matrix and mantling clinopyroxene.

Knockroe intrusive units are ubiquitously, but variably altered (Fig. 3b,c). Alteration minerals include chlorite, prehnite, titanite, magnetite, and calcite (Fig. 4b). Chlorite and calcite are patchily pervasive throughout the units. In many instances magnetite is altered to haematite (Fig. 4d).

Porphyritic dykes

Knockroe porphyritic dykes crosscut Knockroe diatremes, tuffs, lava flows, and hypabyssal intrusions and are composed mainly of plagioclase with lesser amounts of magnetite, minor apatite, and rare clinopyroxene. Plagioclase occurs both as large, subhedral to euhedral phenocrysts and as small, laths that make up most of the matrix. Magnetite is present in the matrix as anhedral to euhedral grains. Apatite is present as subhedral to euhedral lath-like crystals and larger ovoids. Clinopyroxene is rare in these units, but when present it is small and subhedral. These units are often altered to clay minerals and some show pyrite mineralization along their margins (Slezak *et al*., 2023).

Tuffs and agglomerates

The Knockroe unit contains abundant ash and lapilli tuffs, commonly displaying grading, as well as more massive agglomerates (Fig. 3b). The lapilli tuffs and agglomerates consist of angular to sub-angular clasts ranging in size from 200μm up to 1cm in diameter (Fig. 4e). Space between clasts is filled by finer ash and/or calcite (Fig. 4d,e); ash is dominantly altered to clay-rich material. Many of the clasts comprise basaltic material, which may display remnant feldspar phenocrysts (Fig. 4d,e) but are generally almost entirely altered to carbonate and fine-grained white phyllosilicate minerals, chlorite, and clay. Remnant magnetite is ubiquitously oxidised to haematite (Fig. 4d).

Knockseefin units

Intrusions and flows

The Knockseefin unit contains igneous rocks that are alkaline basaltic to basanitic in composition (Slezak *et al*., 2023). The rocks represent hypabyssal intrusions, lava flows, and tuffs (Strogen, 1983). They are dark blue-grey and weakly porphyritic, but overall, relatively fine-grained (Fig. 3d). The rocks contain significant clinopyroxene (Fig. 4f), which typically occurs as euhedral phenocrysts and along with plagioclase comprise the groundmass, with both minerals presenting as subhedral to euhedral laths (Fig. 4f). Indeterminate mafic minerals

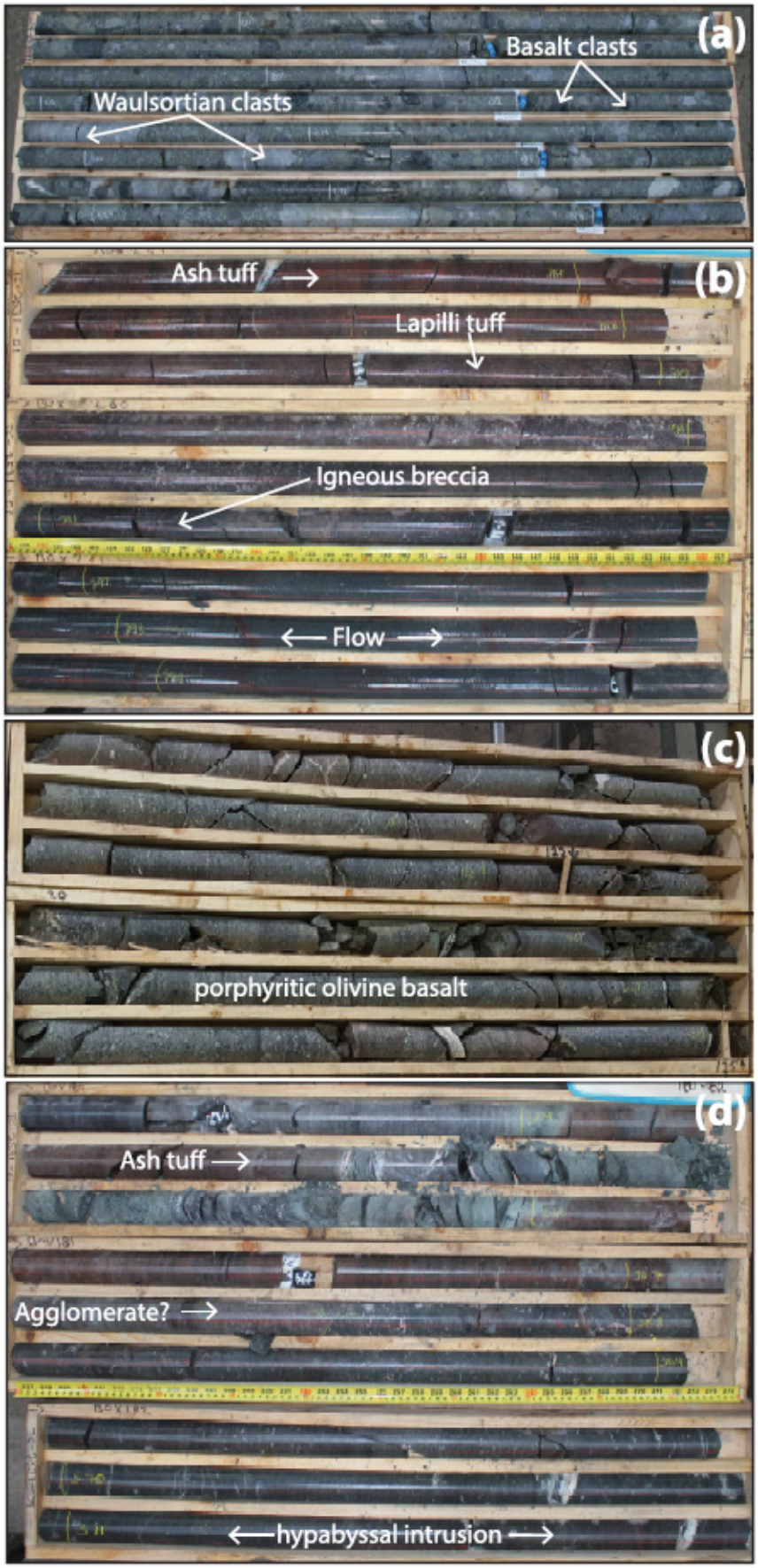

Figure 3: a) *Core from drill hole 2638-28 showing grey-green chlorite-clay altered diatreme material with dark grey basalt and light grey Waulsortian clasts.*

b) *Knockroe ash tuffs, agglomerate, and weakly porphyritic hypabyssal intrusion from drill hole 2531-1.*

c) *Porphyritic olivine-bearing basalt from drill hole 2654-1.*

d) *Core from drill hole 2531-1 illustrating the Knockseefin haematite and chlorite-clay altered ash tuffs, lapilli tuffs, likely flow top breccias, and massive flow material.*

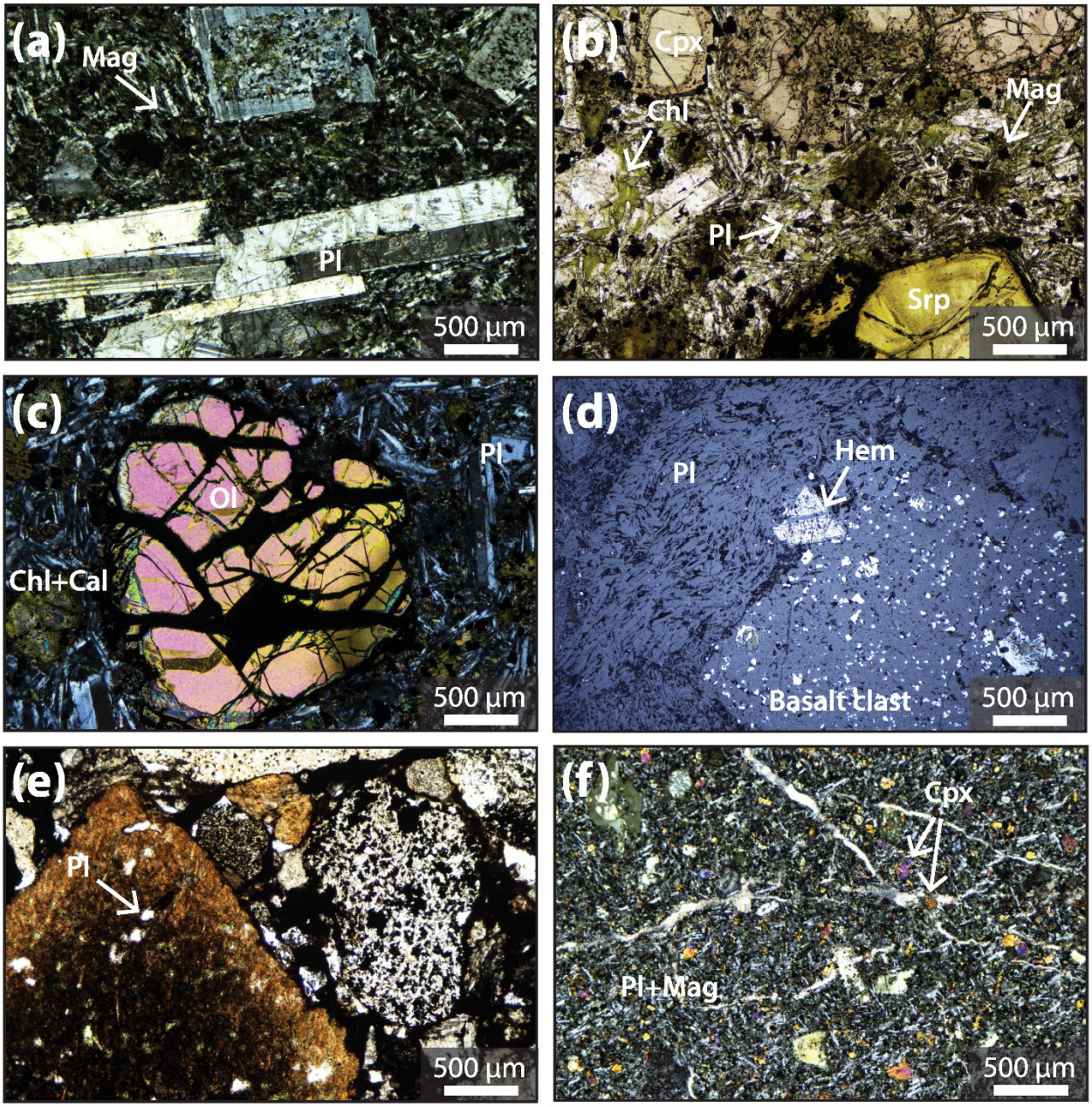

Figure 4: ***a)*** *Cross polarised (XPL) image of plagioclase laths and zoned plagioclase crystal in magnetite-plagioclase matrix from the Knockroe in sample 2531-1-901.* ***b)*** *Plan polarised (PPL) image of zoned clinopyroxene with olivine phenocryst altered to serpentinite and patchy pervasive chlorite alteration from sample 2654-1-123.* ***c)*** *XPL image of sample 2654-1-128 with fractured olivine phenocryst in a plagioclase matrix.* ***d)*** *Reflected light image of oriented plagioclase crystals adjacent to a basalt clast extensively altered to hematite from 2529-491-297.* ***e)*** *PPL image of fine-grained basalt clast altered to hematite with plagioclase phenocrysts from lapilli tuff in sample 2529-491-297.* ***f)*** *XPL image of seriate to weakly porphyritic clinopyroxene in magnetite and plagioclase matrix in Knockseefin sample 2531-1-487. Cal = calcite, Chl = chlorite, Cpx = clinopyroxene, Hem = haematite, Mag = magnetite, Ol = olivine, Pl = plagioclase, Srp = serpentinite*

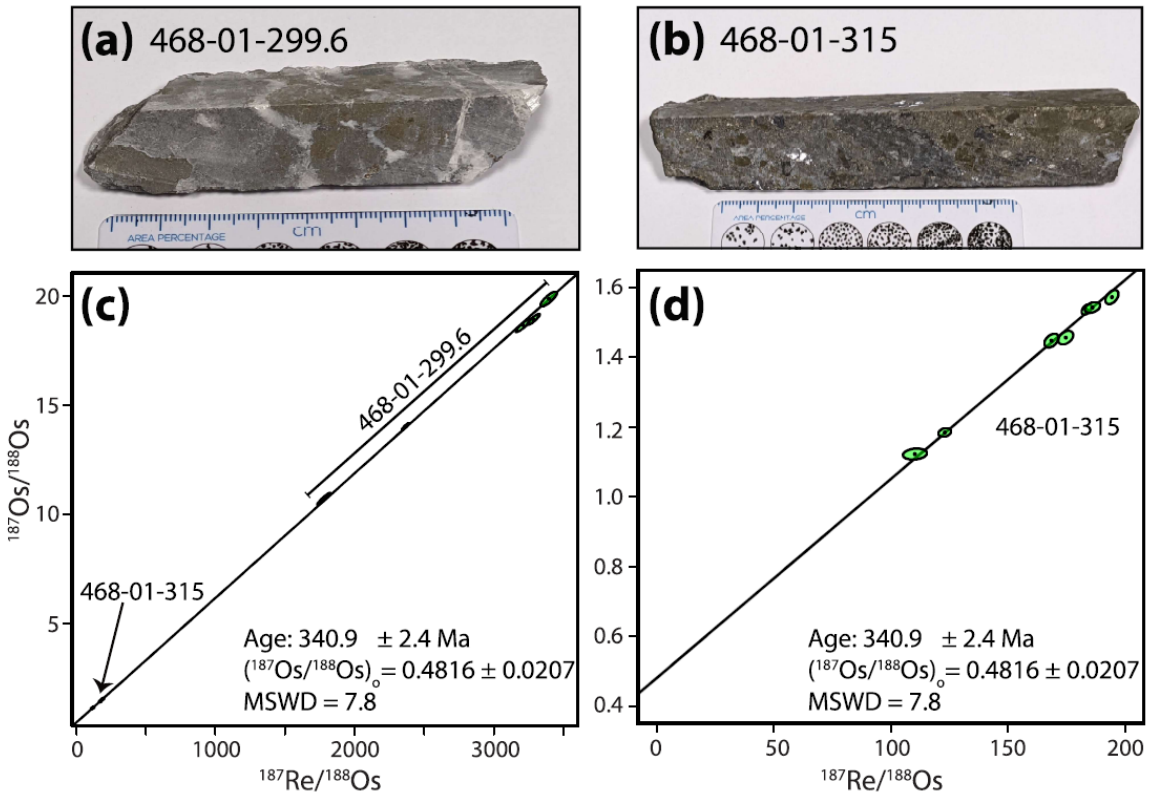

Figure 5: . a) *Sample 468-01-299.6 containing sulphides replacing host carbonates.* ***b)*** *Sample 468-01-315 containing massive pyrite, sphalerite, and galena.* ***c)*** *Combined isochron of samples 448-01-299.6 and 468-01-315.* ***d)*** *A zoomed in view of (c) on sample 468-01-315 to better illustrate isochron data fit.*

(e.g., olivine or orthopyroxene) are occasionally present as large phenocrysts or mineral clots that are altered to serpentinite and iddingsite. Magnetite occurs in the groundmass as small anhedral to subhedral crystals (Fig. 4f). As with the Knockroe units, chlorite, calcite, titanite and prehnite as well as minor serpentinite make up the alteration assemblage.

Tuffs and agglomerates

Extrusive rocks in the Knockseefin unit present as ash and lapilli tuffs in addition to courser agglomerate units (Fig. 3d). The units' thickness and colour as well as grain size and angularity are the same range as the extrusive Knockroe units, making them difficult to distinguish without additional information (e.g., geochemical, geochronological, stratigraphic context, etc.)

Methods

Samples collected for this study were dominantly from diamond drill core and were selected to represent the least altered flow/intrusive rock types as well as the extrusive units. Samples were prepared as polished thin sections and examined using a Nikon Eclipse LV100NPol optical microscope at the Science Foundation Ireland Centre for Research in Applied Geoscience (iCRAG) at University College Dublin (UCD) in Ireland.

Whole rock major and trace element geochemistry

Samples were cut, cleaned, examined for contaminants (e.g., xenoliths) at UCD and sent to ALS Minerals in Loughrea, Co. Galway, Ireland for whole rock major and trace element geochemistry. The samples were analysed according to the methods in Slezak et al., (2023) and data can be found in Appendix A.

Eleven samples were taken from drill hole TC-2531-1 (Appendix A). Sampling began at the base of the Knockroe (near the Lough Gur Formation), continued across the transition from Knockroe to Knockseefin units and finished in the upper sections of least altered Knockseefin intrusive material. Additionally, 3 samples from drill hole G11-2564-1 near Ballywire, Co. Tipperary were sampled as these samples are representative of rare, olivine-bearing Knockroe intrusive units. Lastly, 4 tuffs and 1 diatreme from GC-2529-491 and TC-2638-28, respectively, were sampled and analysed.

Re-Os Sampling and analytical procedures

To determine the timing of base metal mineralization in the Limerick Syncline, we obtained fresh, unaltered sulfides from Group Eleven's G11-468-01 Ballywire drillhole at depths of 299.6m and 315.0m (Fig. 5a, b). Sample 468-01-299.6 is comprised of pyrite and minor sphalerite replacing host carbonate,

Sample Name	Re (ppb)	Re (ppb) 2σ	Os (ppt)	Os (ppt) 2σ	^{187}Re / ^{188}Os	^{187}Re / ^{188}Os 2σ	^{187}Os / ^{188}Os	^{187}Os / ^{188}Os 2σ	Rho
468-01-299.6 M1.9[a]	7.8387	0.0448	50.3329	0.6743	1779.1679	38.3549	10.7115	0.2260	0.9520
468-01-299.6 NM1.9[b]	20.0687	0.1014	102.3078	1.0401	3214.1564	46.1658	18.6371	0.2568	0.9199
468-01-299.6 NM2.0/5[a]	19.6752	0.1211	99.2971	1.1131	3396.4783	49.4758	19.8447	0.2839	0.8421
468-01-299.6 NM2.0/3[b]	18.6388	0.0845	93.9062	0.7576	3285.8405	37.4012	18.9071	0.2051	0.8928
468-01-299.6 NM1.95/2[a]	13.9077	0.0227	79.3545	0.5339	2364.5774	22.7386	14.0132	0.1378	0.9633
468-01-315 NM0.4[b]	0.3055	0.0109	15.0154	0.0658	110.3075	4.1779	1.1224	0.0129	0.1695
468-01-315 NM0.7[b]	0.6885	0.0116	30.5614	0.1002	123.0269	2.2377	1.1843	0.0104	0.2604
468-01-315 NM1.3[b]	1.6575	0.0124	51.2815	0.1543	183.6288	1.7335	1.5364	0.0123	0.4439
468-01-315 NM1.6[b]	1.3028	0.0120	38.2150	0.1508	194.4334	2.2965	1.5717	0.0165	0.4444
468-01-315 NM1.8[b]	1.0056	0.0128	30.7067	0.1034	186.1651	2.6973	1.5421	0.0127	0.3771
468-01-315 NM2.0/5[b]	0.8795	0.0111	28.3451	0.1179	174.7050	2.6234	1.4556	0.0159	0.3872
468-01-315 NM2.0/3[a]	0.9339	0.0111	31.1573	0.1340	168.6110	2.4508	1.4472	0.0162	0.4240

Table 1: *The blank correction used for samples "a" were 4.85 ± 2.26 pg Re and 0.086 ± 0.029 pg Os with a $^{187}Os/^{188}Os$ = 0.51 ± 0.23 (n = 7). The blank correction used for samples "b" were 3.96 ± 2.04 pg Re and 0.101 ± 0.018 pg Os with a $^{187}Os/^{188}Os$ = 0.42 ± 0.12 (n = 6).*

whereas sample 468-01-315 contains massive pyrite, sphalerite, and galena. All samples were crushed to a size 74-210µm using metal-free equipment to prevent metallic contamination and then rinsed with ethanol. Sulphide minerals were extracted from the crushed material via heavy liquid separation using methylene iodide (ρ = 3.32 g/cm^3). The sulphides were then divided into different mineral separates with different magnetic susceptibilities using a Frantz isodynamic separator.

Chemical purification of prepared mineral separates was undertaken at Trinity College Dublin's Clean Geochemistry Laboratory following the isotope dilution procedure of Hnatyshin *et al.* (2016). Isotopic measurements were analysed at the National Centre for Isotope Geochemistry (NCIG) at UCD. All Os isotopic measurements were carried out using negative thermal ionisation mass spectrometry (N-TIMS) on a Thermo-Scientific Triton using the conditions specified in Hnatyshin *et al.* (2016). Rhenium isotopic analysis at UCD were carried out using N-TIMS using the procedures of Hnatyshin *et al*. (2016) or on a Neptune Multi-Collector Inductively Coupled Plasma Mass Spectrometer (MC-ICP-MS) outfitted with 10^{13} Ω amplifiers. Samples were prepared for solution MC-ICP-MS analysis in ~1 M HNO_3 and doped with a standard W solution to be used for mass bias corrections (Poirier & Doucelance, 2009; Dellinger *et al*., 2020). Analysis consisted of utilising a standard bracketing procedure (standard – sample – standard) with the simultaneous measurement of $^{184}W/^{186}W$ and $^{185}Re/^{187}Re$ for online mass bias correction (Miller *et al*., 2009; Dellinger *et al.*, 2020) and then reduced using an in-house data reduction spreadsheet. Ages were calculated using IsoplotR (Vermeesch, 2018) using a Re decay constant of 1.666 x 10^{-11} ± 5.165 x 10^{-14} yr^{-1} (Smoliar *et al*., 1996). Data is presented in Table 1.

Results

LIS geochemistry

The least altered olivine-bearing units from G11-2564-01 plot in the centre of the alkaline basalt field (Fig. 6; Winchester & Floyd, 1977).The additional samples from TC-2531-1, as well as one tuff and the single diatreme sample fall mainly within the alkaline basalt field, whereas other tuff samples fall into the trachyandesite and trachyte fields (Fig. 6). The sample plots follow the two trends (*a* and *b*) presented in Slezak *et al* (2023). Trend *a* shows a general evolution by all rock types, but is especially pronounced in the extrusive units, towards more evolved compositions (e.g. trachyte). Trend b is comprised only of samples from TC-2531-1 and shows a change from alkaline basalts to basanites (Fig. 6).

The MgO and Al_2O_3 contents for the Knockroe units typically range from 2 to 7 wt% and ~13 to ~17 wt%, respectively (Fig. 7a). Compared to the Knockroe, the Knockseefin MgO contents are higher, ranging from 6.5 wt% up to 11 wt% MgO, and the Al_2O_3 values lower (9 to 12 wt% Al_2O_3). Two porphyritic olivine-bearing Knockroe samples (orange in Fig. 7) have MgO values similar to the Knockseefin units (Fig. 7a), but their Al_2O_3 amounts are closer to those observed in the Knockroe. All samples have similar TiO_2 contents (~2.5 to ~4 wt%; Fig. 7b), which is typical of the LIS (Slezak *et al.*, 2023).

For the most part, rocks from the least altered portions of the Knockroe unit have lower Ni contents (e.g., <75 ppm) than those of the Knockseefin unit. The olivine-bearing units are an exception, having Ni contents from 93 to 180 ppm (Fig. 7c and Fig. 8a). These higher values are more in line with the Knockseefin units, which typically have Ni values >145 ppm (Fig. 7c and Fig. 8a; Slezak *et al*., 2023). One Knockseefin sample (TC-2531-1-715) has anomalously low Ni values. The basal Knockroe units typically also have lower Cr in addition to Ni compared to the Knockseefin units higher in the igneous sequence (Fig. 8b). However, Cu and Co contents for both units are variable and not nearly as well constrained to a particular unit type (Fig. 8c,d).

The normalised REY (REE+Y) diagram (Fig. 9a) shows the least altered Knockroe and Knockseefin units from TC-2531-1 as well as the olivine-bearing samples display patterns similar to Oceanic Island Basalts ('OIB') (Sun & McDonough, 1989) with downward sloping patterns, minimal distinctives tetrad shapes (e.g., Masuda *et al.*, 1987), and a very slight negative Y anomaly. The olivine-bearing Knockroe samples have

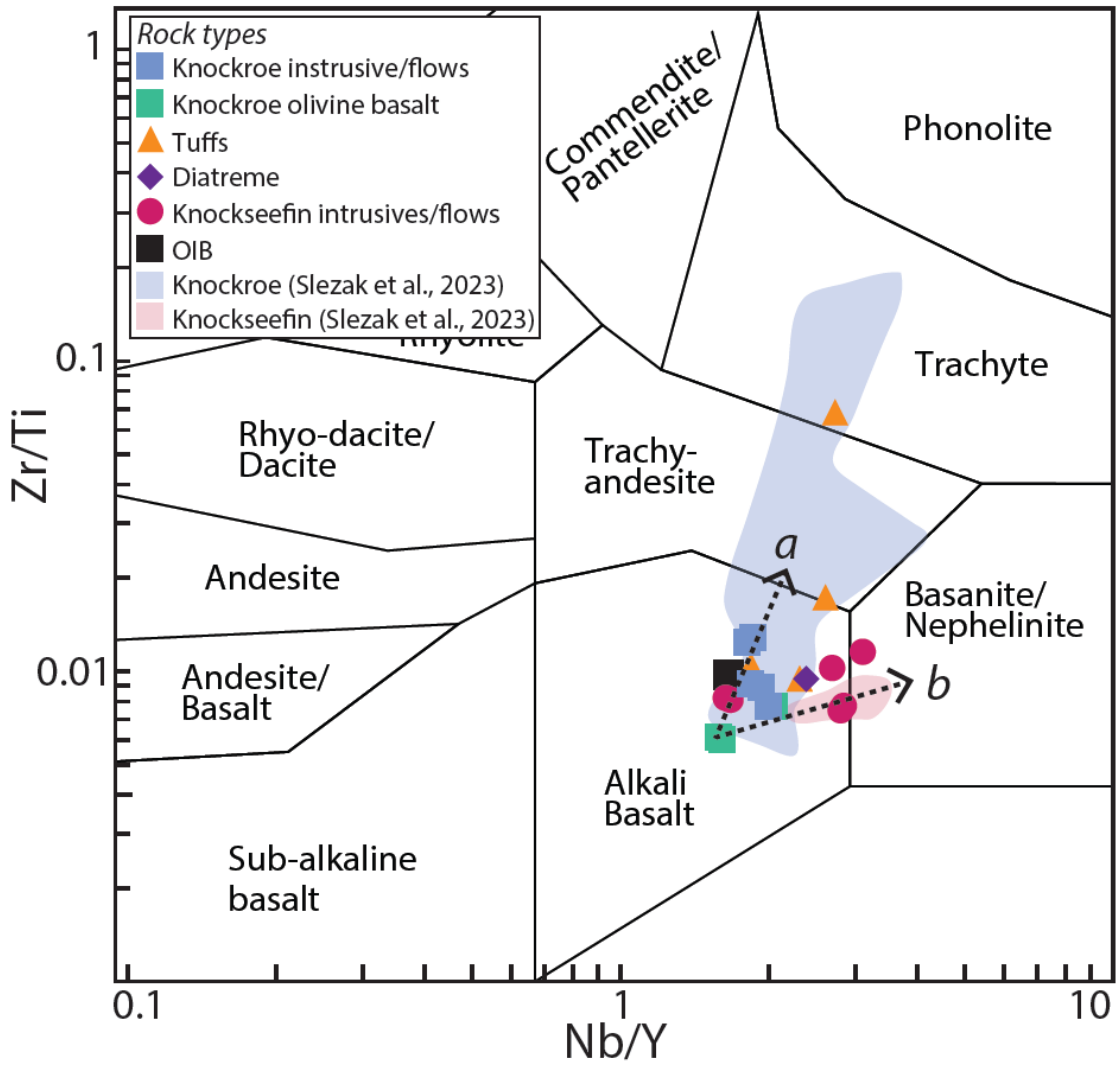

Figure 6: *Trace element diagramme for volcanic rocks (from Winchester & Floyd, 1977). Note trends a and b from Slezak et al. (2023) have been extended to include the porphyritic olivine samples.*

slightly lower normalised REY values compared to OIB, but the overall patterns compared to the other LIS units are nearly identical (Fig. 9a). The patterns for the tuff and diatreme samples are more variable than the intrusive units, likely due to their variable alteration (Fig. 9b). Though most extrusive samples are similar to their intrusive counterparts, one trachytic tuff sample shows a distinct negative Eu anomaly (Fig. 9b).

Re–Os ages

A compilation of the Re–Os data is provided in Table 1. A total of 7 datapoints comprised of pyrite, sphalerite, and galena mineral separates from sample 468-01-315 (Fig. 5b) were analysed and contained between 0.3-1.7 ppb Re and 15-51 ppt Os. Another 5 datapoints from pyrite and sphalerite mineral separates from sample 468-01-299.6 (Fig. 5a) contained 8-20 ppb Re and 50-102 ppt Os. A model 1 isochron age of 340.9 ± 2.4 Ma (MSWD = 7.8) with an initial $^{187}Os/^{188}Os$ of 0.48 ± 0.02 (Fig. 5c,d) is created by combining these 12 datapoints.

Discussion

Porphyritic, olivine-bearing basalt origins

The least altered intrusive and flow units of the Knockroe units are mainly alkaline basalt evolving towards trachyandesites (Trend *a*; Fig. 6) whereas the Knockseefin units are alkaline basalts and basanites (Trend *b*; Fig. 6). Slezak *et al.* (2023) showed that the Knockroe and Knockseefin units are genetically related based on their similar normalised trace element plots, similar Nd isotope ratios, and nearly identical Sr isotope ratios. Furthermore, the change in rock type from alkaline basalt to basanite is likely a function of the degree of partial melting (Fig. 7d) as units with higher Zr/Nb and lower Ce/Y are indicative of magmas that have undergone higher degrees of partial melting (Kay & Gast, 1973; Smedley, 1988). Trace element contents of Ni and Cr (Fig. 7c and Fig. 8a,b) are generally higher in the Knockseefin units than in the Knockroe units, but deviations from this (Fig. 8a,b) suggest that the change from Knockseefin to Knockroe, and consequently shift from

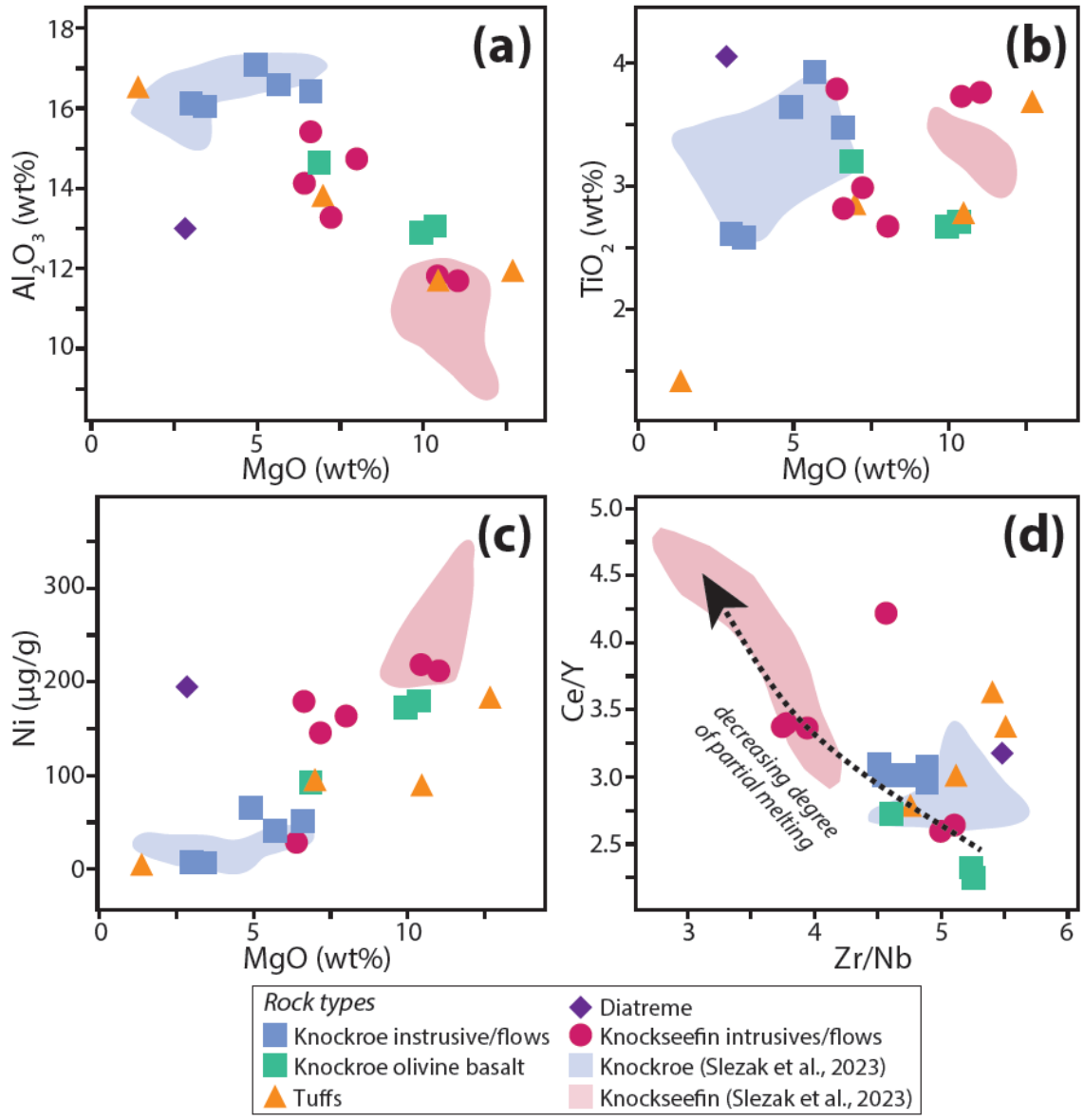

Figure 7: *X-Y diagrammes for major and trace elements for the tuffs, diatreme, olivine-bearing basalt samples as well as least altered Knockroe and Knockseefin intrusive units.*

alkaline basalt to basanite, may not have been an abrupt change. Rather, there was likely a sporadic change with low degrees of partial melting becoming more common resulting in the shift from alkaline basalt to basanite observed in Trend *b* (Fig. 6).

Although olivine is rarely observed in the LIS, this study demonstrates that porphyritic, olivine-bearing basalts near the Ballywire deposit (Fig. 2) plot in the alkaline basalt field at a vergence between Trends *a* and *b* (Fig. 6). These units are slightly less enriched in trace elements (e.g., REE) compared to other Knockroe and Knockseefin units; however, their patterns are nearly identical to the LIS units, which also strongly correspond to OIB trace element signatures (Fig. 9). Based on their trace element patterns and potential to represent the highest degree of partial melting (Fig. 7d) relative to the other Knockroe and Knockseefin units, these olivine-bearing basalts may represent an early phase of alkaline basalts in LIS.

Volcanic unit connections

The ash and lapilli tuffs and agglomerates in the Limerick Syncline are interbedded with the flows and hypabyssal intrusions (Fig. 3) with the diatremes having a complex cross cutting relationship with the other units (Elliott *et al.*, 2015). The tuffs have similar, albeit more varied trace element patterns compared to the least altered units (Fig. 8; Slezak *et al.*, 2023), and two tuffs and the diatreme sample plot within the same fields (see Fig. 6) as the massive flow and hypabyssal intrusive units from the Knockroe, suggesting a common source for both intrusive and extrusive units.

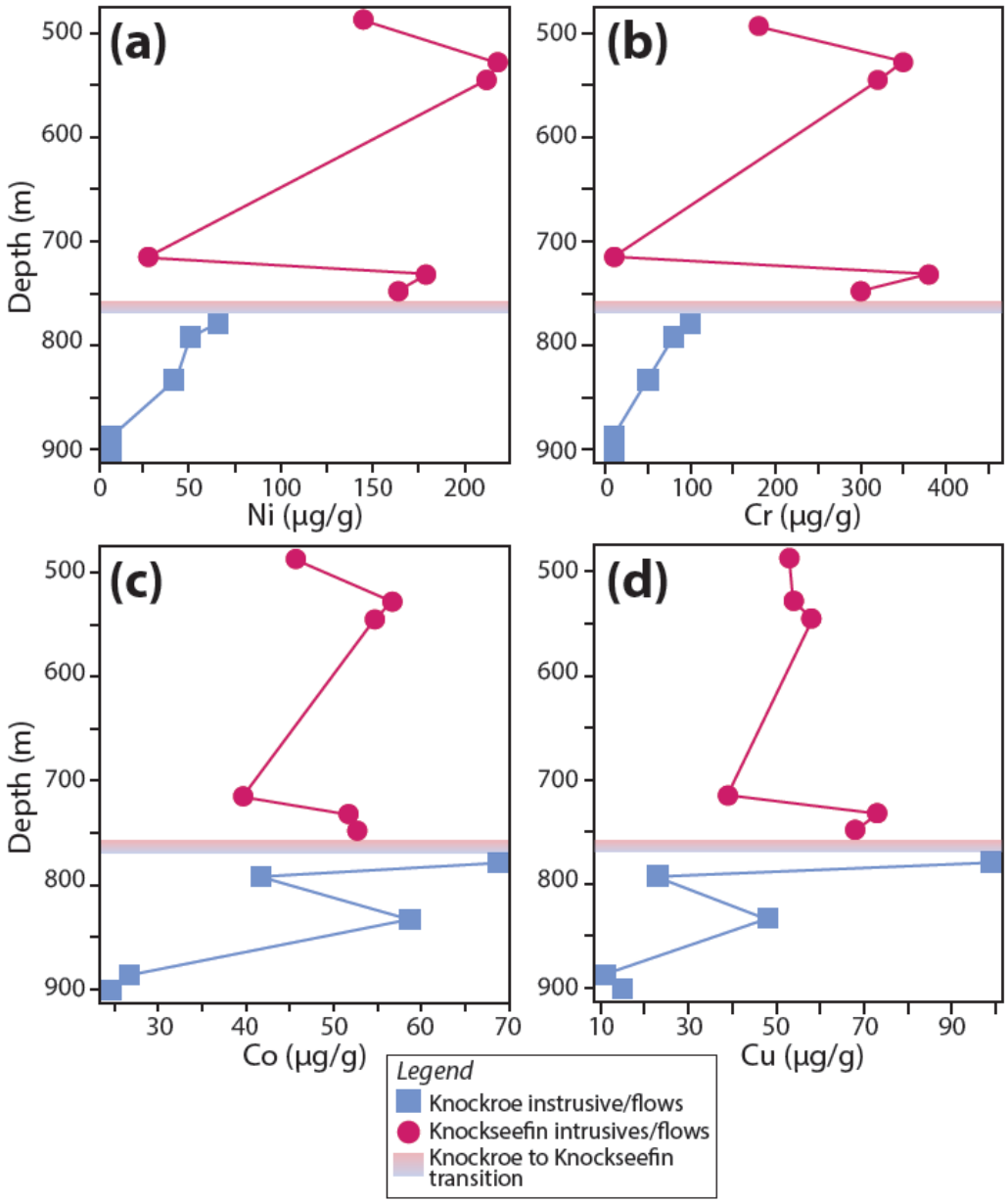

Figure 8: *Downhole plots of the trace elements Ni, Cr, Co, and Cu for TC-2531-1. Note the authors identified the change from Knockseefin to Knockroe based on visual and geochemical data. The transition consists of a volcaniclastic unit that separates the two units.*

However, the tuffs in both areas exhibit larger negative Eu anomalies than the intrusive LIS units from this study (Fig. 8) as well as some of the units discussed in Slezak *et al.* (2023). In addition, Koch (2021) demonstrated that apatite derived from volcanic tuffs found near base metal deposits in the Rathdowney Trend evolved along a similar, but more extensive trend compared to the igneous apatite from Slezak *et al.* (2023), suggesting that some of these volcanic apatite may have been derived from more evolved units. Bulk rock geochemistry from the extrusive units also suggests that some of the extrusive units may be slightly more evolved, plotting towards the trachyandesite and trachyte fields (Fig. 6). However, these extrusive units tend to be significantly altered and it is important to note that Slezak *et al.* (2023) demonstrated that Ti mobility related to magnetite alteration and decomposition is likely responsible for at least some of the most evolved igneous data previously reported in the LIS (see Strogen, 1988 and Elliot *et al.*, 2015).

Ages and links to mineralization

Within the Limerick Syncline there is a clear spatial correlation between base metal mineralization and the presence of igneous material (e.g., McCusker & Reed, 2013; Kerr, 2015; Elliott *et al.*, 2019; Slezak *et al.*, 2023); however, a temporal and ultimately genetic relationship is less clear. The major igneous

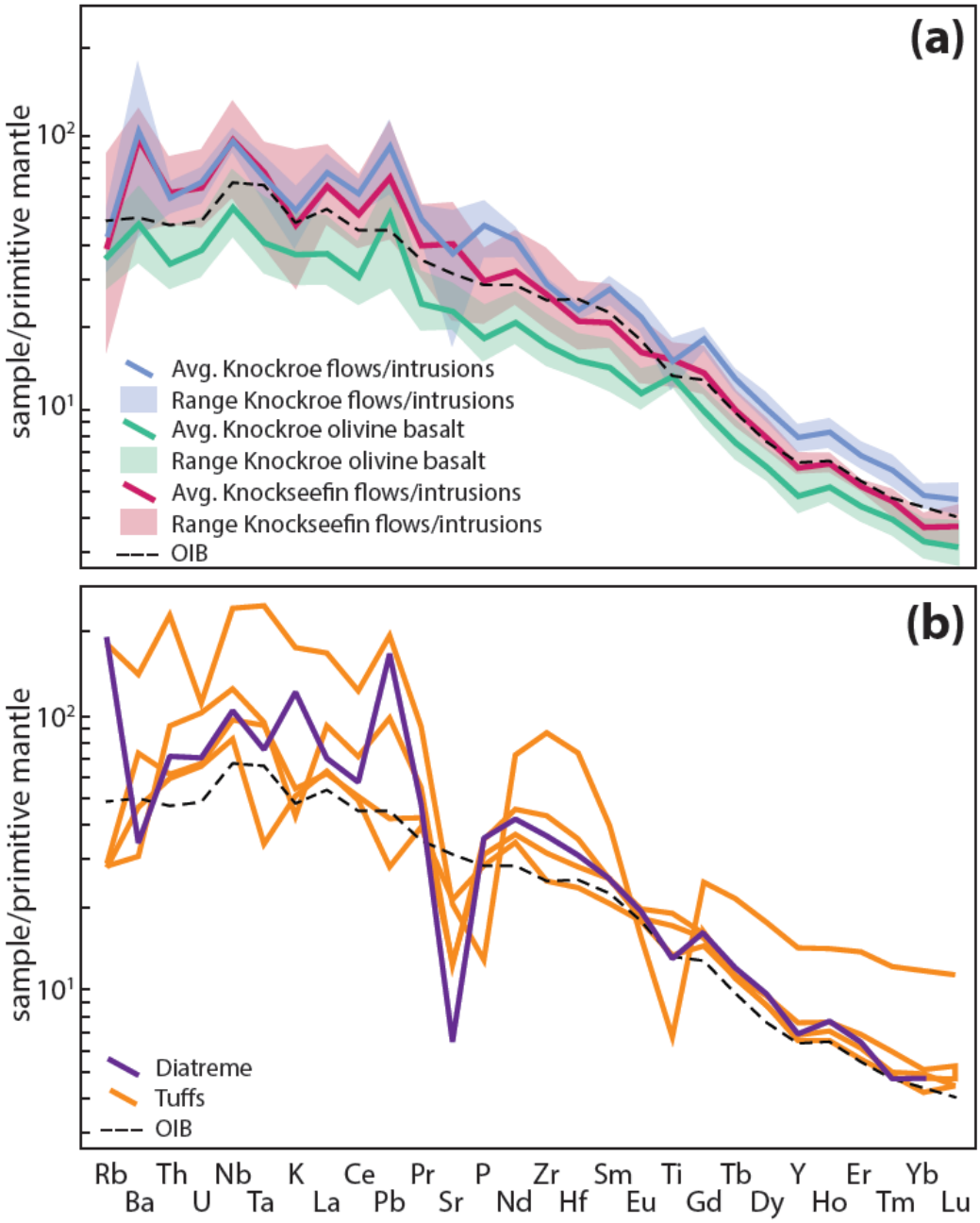

Figure 9: *Primitive mantle-normalised trace element diagramme (Sun & McDonough, 1989) for a) least altered Knockroe and Knockseefin flows/hypabyssal intrusions as well as the olivine-bearing basalts, and b) diatreme and tuff samples.*

activity in the LIS is directly constrained from apatite extracted from the intrusive Knockroe alkaline basalts and trachytic dykes, which have magmatic ages of 353 ± 6 Ma and 349 ± 5 Ma, respectively (Slezak *et al*., 2023). These geochemical ages move the Knockroe units into the lower Viséan/Upper Tournaisian, which is older than previous biostratigraphy work would suggest (e.g., Somerville *et al*., 1992). Ages for the Knockseefin were not able to be determined. Presently, biostratigraphy places the Knockseefin unit emplacement from ~341 to 333 Ma (i.e., Arundian to Late Asbian; Somerville *et al*., 1992) with a median age of ~337 Ma assumed for isotopic analyses (e.g. Slezak *et al*., 2023).

The timing of base-metal mineralization along the Iapetus Suture Zone (ISZ) is constrained by sulphide Re–Os ages of 346.6 ± 3.0 Ma and 334.0 ± 6.1 Ma for the Lisheen Mine and Silvermines deposit, respectively (Hnatyshin *et al*., 2015). The Silvermines age was further corroborated by a hydrothermal apatite U–Pb age of 331.0 ± 5.6 Ma (Vafeas *et al*., 2023). The 340.9 ± 2.4 Ma date produced from this study (Fig. 5c, d) for

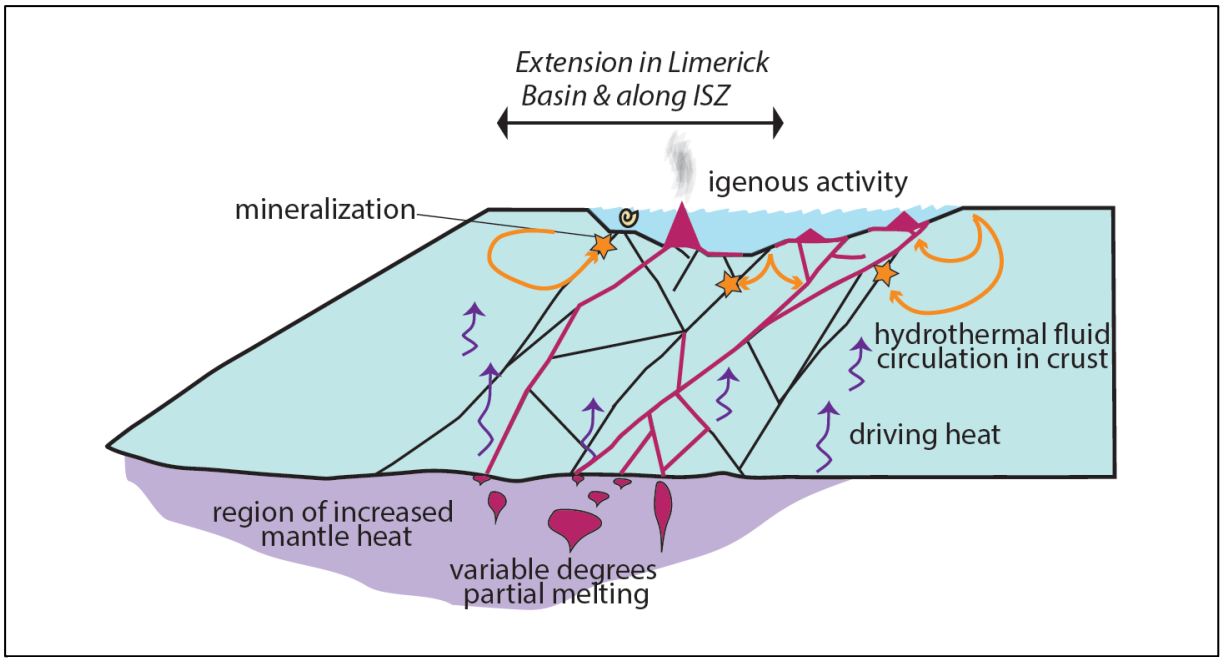

Figure 10: *Genetic model illustrating increased mantle heat and heat from LIS emplacement as a potential driver for hydrothermalism along the ISZ. Note that mineral deposits/occurrences are not likely to occur in the same locations as igneous material.*

the Ballywire prospect (Fig. 2) represents the first date for carbonate-hosted base metal mineralization closely associated with igneous bodies in Ireland and broadly aligns with previously reported ages from Hnatyshin *et al.* (2015). The Ballywire age is younger than that of the Knockroe intrusive units but is within the biostratigraphic age range of the Knockseefin and overlaps in age with several regional tuff ages (Koch, 2021).

Despite the contemporaneous emplacement of the LIS and base metal mineralization, we propose that the igneous activity from the LIS was not the source for the metals in Irish-type deposits based on several geochemical arguments. The precise value for the initial $^{187}Os/^{188}Os$ from Ballywire (0.48 ± 0.02) reflects the potential source of Os in the fluids that resulted in mineralization. Mantle derived sources will be ~0.13 (Meisel *et al*., 2001), whereas crustal sources are expected to be much higher. The Ballywire $^{187}Os/^{188}Os$ of 0.48 ± 0.02 is nearly identical to the much younger (334.0 ± 6.1 Ma) Silvermines deposit which has a value of 0.45 ± 0.01, suggesting a very similar source for Os. Hnatyshin *et al.* (2015) calculated that the most likely source of Os based on the observed initial $^{187}Os/^{188}Os$ from Lisheen and Silvermines was the early Palaeozoic basement rather than an igneous source. By extension, even though the Ballywire mineralization is closely spatially associated with the Knockroe igneous units, there is no indication the Os is sourced from anything other than basement rock, or potentially another crustal source.

Slezak *et al.* (2023) showed that the LIS has a slightly enriched, but clearly mantle source based on Sr and Nd isotope values (e.g., $^{87}Sr/^{86}Sr_{(t)}$ = 0.70301 – 0.70454 and $^{143}Nd/^{144}Nd_{(t)}$ = 0.512457 – 0.512493 for the least altered Knockroe units). Furthermore, Slezak *et al*. (2023) conducted isotope mixing models and were unable to reconcile the positive εNd isotope values (e.g., $\varepsilon Nd_{(t)}$ = +4.15 to +4.55 for the Knockseefin units) compared to the negative, crustal εNd values (e.g. $\varepsilon Nd_{(t)}$ = -8.4 to -12.2) reported for Irish-type deposit ore fluid proxies in Walshaw *et al.* (2006). Moreover, recent work by Cordeiro *et al*. (2023) showed that Sr and Nd isotopes from the Gortdrum Mine had negative εNd values (e.g., $\varepsilon Nd_{(t)}$ = -5.56 to -7.44) and high Sr ratios (e.g., $^{87}Sr/^{86}Sr_{(t)}$ = 0.07076 – 0.71150) in line with crustal sources including the Waulsortian limestones, Old Red Sandstone, and other Silurian sedimentary rocks, further suggesting a significant crustal component to the base metal mineralization in the Limerick Syncline.

Genetic Model

Though the LIS may not be a base-metal source, $\delta^{34}S$ values would allow some igneous component (Hitzman & Beaty, 1996; Wilkinson *et al*., 2005a,b). Additionally, He isotope studies from Davidheiser-Kroll *et al.* (2014) showed that the ore fluids from Silvermines, Galmoy, and Lisheen had slightly elevated $^{3}He/^{4}He$ values of 0.15–0.2 R_a, suggesting a small amount of mantle input. We suggest the heat generated by LIS activity itself, and potentially any increased mantle heat flux that led to partial mantle melting and the LIS emplacement, may have been a driver for hydrothermalism (Fig. 10), which ultimately helped facilitate base-metal emplacement in SW Ireland.

McCusker & Reed (2013) noted a distinct lack of feeder faults in the Limerick Syncline to facilitate fluid mobility. Blaney and Coffey (this volume) present evidence that sulphide mineralization crosscut and overprinted LIS igneous material, not only suggesting that sulphides mineralization was likely post-igneous emplacement but also that the igneous material was hindering rather facilitating mineralization. Given the ubiquity of alteration present in the LIS (see Slezak *et al*., 2023), the

disparity in mineralization styles in the Limerick Syncline, and lack of identifiable feeder faults (McCusker & Reed, 2013), it is likely that some of the LIS units likely acted as hydrothermal aquitards, blocking fluid pathways (i.e., faults), and causing wider dispersal of base-metal fluids throughout the basin (Fig. 10).

Prior to partial melting from the mantle, the LIS units likely would have moved through the crust via deep-seated faults related to extension along the ISZ (Murphy *et al.*, 2011; Kroner & Romer, 2013; Smit *et al.*, 2018). As they reached near-surface levels, they would have interacted with seawater, causing diatreme like eruptions followed by emplacement of hypabyssal intrusions and flows in the shallow subsurface and along the ocean floor, respectively. Continued emplacement would have then occurred along subordinate fault networks, leading dyke emplacement, such as those found near the historic Oola copper mine (Fig. 1; Steed, 1975) and hindering hydrothermal fluid migration. As magmatism progressed, the LIS activity became volcanic, causing submarine and subaerial eruptions, potentially similar to Surtseyan volcanism (Vestmannaeyjar, Iceland) (Schipper *et al.*, 2015 and references therein).

Conclusions

- The LIS is composed of a variety of units, with the extrusive tuffs, agglomerates, and diatremes being geochemically akin to their intrusive counterparts.
- The recently described porphyritic olivine basalt is geochemically similar to the least altered Knockroe units and may represent the highest degree of partial melting within the LIS.
- The sulphide age of 340.9 ± 2.4 Ma from the Ballywire prospect represents the first known mineralization age in the Limerick Syncline.
- The $^{187}Os/^{188}Os$ of 0.48 ± 0.02 is indicative of crustal sources for base metals, suggesting the LIS is not the source of metals in the Limerick Syncline
- The heat generated by LIS emplacement potentially facilitated hydrothermalism, but the LIS units may have acted as aquitards, dispersing mineralizing fluids rather than concentrating them.

Acknowledgements

This publication has emanated from research conducted with the financial support of Science Foundation Ireland (SFI) under grant number numbers 16/RP/3849 and 13/RC/2092_P2, awarded to Murray W. Hitzman. We thank Group Eleven Resource and Glencore for their hospitality while conducting field work and core logging. Lastly, we thank Colin Andrew for his editorial handling.

References

Ashton, J.H., Andrew, C.J. & Hitzman, M.W. (2023) Irish type Zn-Pb deposits (Its) – What are they and can we find more? This volume.

Blaney, D. & Coffey, E. (2023) The volcano-stratigraphic setting of the Pallas Green zinc-lead deposit, County Limerick. This volume.

Chew, D.M. & Stillman, C.J. (2009) Late Caledonian orogeny and magmatism. In: Holland, C.H. and Sanders, I.S. (eds) *The Geology of Ireland*. Dunedin Academic Press, Edinburgh, Scotland, 143–173.

Chew, D.M., Babechuk, M.G., Cogné, N., Mark, C., O'Sullivan, G., Henrichs, I.A., Doepke, D. & McKenna, C.A. (2016) (LA,Q)-ICPMS trace-element analyses of Durango and McClure Mountain apatite and implications for making natural LA-ICPMS mineral standards. *Chemical Geology*, v.435, 35–48,

Cordeiro, P.M., Santos, A.M.d.S., Steed, G., Silva, A.d.A., Meere, P., Corcoran, L., Simonetti, A. & Unitt, R. (2023) The carbonate-hosted Gortdrum Cu-Ag(±Sb-Hg) deposit, SW Ireland: C-O-Sr-Nd isotopes and whole-rock geochemical signatures. *Journal of Geochemical Exploration*, v.248, 107196,

Davidheiser-Kroll, B., Stuart, F., & Boyce, A. (2014) Mantle heat drives hydrothermal fluids responsible for carbonate-hosted base metal deposits: Evidence from $^{3}He/^{4}He$ of ore fluids in the Irish Pb-Zn ore district. *Mineralium Deposita*, v.49, 547–553,

Dellinger, M., Hilton, R.G. & Nowell, G.M. (2020) Measurements of rhenium isotopic composition in low-abundance samples. Journal of *Analytical Atomic Spectrometry*, v.35, 2, 377–387,

Devuyst, F.X. & Lees, A. (2001) The initiation of Waulsortian build-ups in Western Ireland. *Sedimentology,* v.48, 1121–1148,

Elliott, H.A.L., Gernon, T.M., Roberts, S. & Hewson, C. (2015) Basaltic maar diatreme volcanism in the Lower Carboniferous of the Limerick Basin (SW Ireland). *Bulletin of Volcanology,* v.77, 37,

Elliott, H.A.L. (2015) Pb-Zn Mineralization Within the Limerick Basin (SW Ireland): A Role for Volcanism? PhD Thesis, University of Southampton, 198.

Elliott, H.A.L., Gernon, T.M., Roberts, S., Boyce, A.J. & Hewson, C. (2019) Diatremes act as fluid conduits for Zn-Pb mineralization in the SW Irish ore field. *Economic Geology*, v.114, 117–125,

Graham, J.R. (2009) Devonian. In: Holland, C.H. and Sanders, I.S. (eds) *The Geology of Ireland*. Dunedin Academic Press, Edinburgh, Scotland, 175–214.

Hitzman, M.W. & Beaty, D.W. (1996) The Irish Zn-Pb-(Ba) orefield. *Society of Economic Geologists, Special Publication* v.4, 112–143,

Hitzman, M.W., Beaty, D.W., & Redmond, P. (2002) The carbonate-hosted Lisheen Zn-Pb-Ag deposit, Co. Tipperary, Ireland. *Economic Geology*, v.97, 1627–1655,

Hnatyshin, D., Creaser, R.A., Wilkinson, J.J. & Gleeson, S.A. (2015) Re-Os dating of pyrite confirms an early diagenetic onset and extended duration of mineralization in the Irish Zn-Pb ore field. *Geology,* v.43, 143–146.

Hnatyshin, D., Kontak, D.J., Turner, E.C., Creaser, R.A., Morden, R., & Stern, R.A. (2016) Geochronologic (Re-Os) and fluid-chemical constraints on the formation of the Mesoproterozoic-hosted Nanisivik ZnPb deposit, Nunavut, Canada: Evidence for early diagenetic, low-temperature conditions of formation. *Ore Geology Reviews,* v.79, 189–217,

Kay, R.W. & Gast, P.W. (1973) The rare earth content and origin of alkali-rich basalts. *Journal of Geology,* v.81, 653–682,

Kerr, N. (2013) Geology of the Stonepark Zn-Pb prospects, County Limerick, Ireland. MSc thesis, Colorado School of Mines, 118 p.

Koch, H.A. (2021) Chemostratigraphic Investigation of Early Carboniferous Tuffs and Limestones from the Irish Midlands Based on

Geochemical and Geochronological Fingerprinting. PhD thesis, Trinity College Dublin, 304 p.

Kroner, U. & Romer, R.L. (2013) Two plates – many subduction zones: the Variscan orogeny reconsidered. *Gondwana Research*, v.24, 298–329,

Masuda, A., Kawakami, O., Dohmoto, Y.& Takenaka, T. (1987) Lanthanide tetrad effects in nature: two mutually opposite types, W and M. *Geochemical Journal*, v.21, 119–124,

McConnell, B., Riggs, N. & Fritschle, T. (2021) Tectonic history across the Iapetus suture zone in Ireland. *Geological Society, London, Special Publications,* 333–345,

McCusker, J. & Reed, C. (2013) The role of intrusions in the formation of Irish-type mineralization. *Mineralium Deposita*, v.48, 687–695,

Meisel, T., Walker, R.J., Irving, A.J., & Lorand, J.-P. (2001) Osmium isotopic compositions of mantle xenoliths: A global perspective. *Geochimica et Cosmochimica Acta,* v.65, 1311–1323,

Miller, C.A., Peucker-Ehrenbrink, B., & Ball, L. (2009) Precise determination of rhenium isotope composition by multi-collector inductively-coupled plasma mass spectrometry. *Journal of Analytical Atomic Spectrometry,* v.24, 8, 1069–1078,

Murphy, J.B., Waldron, J.W.F., Kontak, D.J., Pe-Piper, G. & Piper, D.J.W. (2011) Minas fault zone: late Paleozoic history of an intra-continental orogenic transform fault in the Canadian Appalachians. *Journal of Structural Geology*,v.33, 312–328,

O'Rourke, H. (2013)A U-Pb Zircon Study of Granulite-Facies Xenoliths Hosted by Lower Carboniferous Volcanic Diatremes from Limerick, South-West Ireland. MSc thesis. University College Dublin.

Poirier, A., & Doucelance, R. (2009) Effective Correction of Mass Bias for Rhenium Measurements by MC-ICP-MS. *Geostandards and Geoanalytical Research*, v.33, 2, 195–204,

Sakai, H., Marais, D.J.D., Ueda, A., & Moore, J.G. (1984) Concentrations and isotope ratios of carbon, nitrogen and sulfur in ocean-floor basalts. *Geochimica et Cosmochimica Acta,* 48, 2433–2441,

Schipper, C.I., Jakobsson, S.P., White, J.D.L., Palin, J.M., & Bush-Marcinowski, T. (2015) The Surtsey Magma Series. *Scientific Reports*, v.5,11498,

Seal, R.R., II. (2006) Sulfur Isotope Geochemistry of Sulfide Minerals. *Reviews in Mineralogy and Geochemistry*, 61, 633-677,

Sevastopulo, G.D. & Wyse Jackson, P.N. (2009) Carboniferous: Mississippian (Serpukhovian and Pennsylvanian). In: Holland, C.H. and Sanders, I.S. (eds) *The Geology of Ireland*. Dunedin Academic Press, Edinburgh, Scotland, 269–294.

Slezak P., Hitzman M.W., van Acken D., Dunlevy E., Chew D., Drakou F., & Holdstock M. (2023) Petrogenesis of the Limerick Igneous Suite: insights into the causes of post-eruptive alteration and the magmatic sources underlying the Iapetus Suture in SW Ireland: *Journal of the Geological Society*, v.180,

Smedley, P.L. (1988) Trace element and isotopic variations in Scottish and Irish Dinantian volcanism: evidence for an OIB-like mantle source. *Journal of Petrology*, v.29, 413–443,

Smit, J., van Wees, J.-D. & Cloetingh, S. (2018) Early Carboniferous extension in East Avalonia: 350 My record of lithospheric memory. *Marine and Petroleum Geology*, 92, 1010–1027,

Smoliar, M.I., Walker, R.J., & Morgan, J.W. (1996) Re-Os Ages of Group IIA, IIIA, IVA, and IVB Iron Meteorites. *Science,* v.271, 5252, 1099–1102,

Somerville, I.D., Strogen, P., & Jones, G.L. (1992) The biostratigraphy of Dinantian limestones and associated volcanic rocks in the Limerick Syncline, Ireland. *Geological Journal,* v.27, 201–220,

Somerville, I.D., Waters, C.N., & Collinson, J.D. (2011) South Central Ireland. In: Waters, C.N., Somerville, I.D., Jones, N.S., Cleal, C.J., Collinson, J.D., Waters, R.A., Besly, B.M., Dean, M.T., Stephenson, M.H., Davies, J.R., Freshney, E.C., Jackson, D.I., Mitchell, W.I., Powell, J.H., Barclay, W.J., Browne, M.A.E., Leveridge, B.E., Long, S.L., McLean, D. (eds) A Revised Correlation of Carboniferous Rocks in the British Isles. *Geological Society of London*, pp. 144–152.

Steed, G.M. (1975) The Geology and Mineralization of the Gortdrum District. PhD Thesis, University of London, 332 p.

Strogen, P. (1983) The Geology of the Volcanic Rocks of Southeast County Limerick. PhD Thesis, University College Dublin, 609 p.

Strogen, P. (1988) The Carboniferous lithostratigraphy of southeast County Limerick, Ireland and the origin of the Shannon Trough. *Geological Journal,* v.23, 121–137,

Strogen, P. & Somerville, I.D. (1984) The stratigraphy of the Upper Palaeozoic rocks of the Lyons Hill area, Co. Kildare. *Irish Journal of Earth Sciences*, v.6, 155–173,

Sun, S.S & McDonough, W.F. (1989) Chemical and isotopic systematics of oceanic basalts: implications for mantle composition and processes. *Geological Society, London, Special Publications,* v.42, 313–345,

Vafeas N.A., Slezak .P, Chew D., Brodbeck M., Hitzman M.W., & Hnatyshin D. (2023) U-Pb Dating of apatite from Silvermines deposit, Ireland: a model for hydrothermal ore genesis. *Economic Geology*, In Press

Van den Berg, R., Daly, J.S. & Salisbury, M.H. (2005) Seismic velocities of granulite-facies xenoliths from Central Ireland: implications for lower crustal composition and anisotropy. Tectonophysics, v.407, 81–99,

Vaughan, A.P.M. & Johnston, J.D. (1992) Structural constraints on closure geometry across the Iapetus suture in eastern Ireland. *Journal of the Geological Society* v.149, 65–74.

Vermeesch, P. (2018) IsoplotR: A free and open toolbox for geochronology. *Geoscience Frontiers*, v.9, 1479–1493,

Walshaw, R.D., Menuge, J.F. & Tyrrell, S. (2006) Metal sources of the Navan carbonate-hosted base metal deposit, Ireland: Nd and Sr isotope evidence for deep hydrothermal convection. *Mineralium Deposita,* v.41, 803–819,

Wilkinson, J.J., Eyre, S.L., & Boyce, A.J. (2005a) Ore-forming processes in Irish-type carbonate-hosted Zn-Pb deposits: Evidence from mineralogy, chemistry, and isotopic composition of sulfides at the Lisheen Mine. *Economic Geology* v.100, 63–86,

Wilkinson, J.J., Everett, C.E., Boyce, A.J., Gleeson, S.A., & Rye D.M. (2005b) Intracratonic crustal seawater circulation and the genesis of subseafloor zinc-lead mineralization in the Irish orefield. *Geology,* v.33, 805–808.

Wilkinson, J.J. & Hitzman, M.W. (2015) The Irish Zn-Pb Orefield: The View from 2014. In: Archibald, S.M. and Piercey, S.J. (eds.) Current perspectives on zinc deposits. *Irish Association of Economic Geology, Special Publicatio*n, 59–72.

Winchester, J.A. & Floyd, P.A. (1977) Geochemical discrimination of different magma series and their differentiation products using immobile elements. *Chemical Geology*, v.20, 325–343.

Appendix A. Bulk rock geochemical data.

Sample	Unit	Description	Alteration	Easting ITM	Northing ITM	SiO2	TiO2	Al2O3	Fe2O3	MnO	MgO	CaO	Na2O	K2O	P2O5
						%	%	%	%	%	%	%	%	%	%
2531-1-487	Knockseefin	hyp. Int/flow	least altered	564468	644731	42.92	2.99	13.27	13.46	0.17	7.2	11	2.78	1.52	0.74
2531-1-528	Knockseefin	hyp. Int/flow	least altered	564468	644731	40.82	3.73	11.82	14.47	0.2	10.45	11	2.05	0.84	0.67
2531-1-545	Knockseefin	hyp. Int/flow	least altered	564468	644731	40.48	3.76	11.72	14.53	0.2	11.05	11.1	1.54	1.09	0.68
2531-1-715	Knockseefin	hyp. Int/flow	least altered	564468	644731	43.14	3.79	14.14	14.95	0.24	6.41	8.52	1.92	2.69	0.84
2531-1-732	Knockseefin	hyp. Int/flow	least altered	564468	644731	44.8	2.82	15.4	14.16	0.33	6.63	9.04	2.71	1.22	0.47
2531-1-748	Knockseefin	hyp. Int/flow	least altered	564468	644731	44.7	2.68	14.73	13.59	0.24	8.02	8.87	2.14	1.18	0.45
2531-1-779	Knockroe	hyp. Int/flow	least altered	564468	644731	48.82	3.65	17.13	10.2	0.25	4.93	3.9	5.75	1.18	0.93
2531-1-792	Knockroe	porph int	least altered	564468	644731	44.61	3.48	16.42	12.61	0.41	6.59	5.3	4.14	1.54	0.93
2531-1-833	Knockroe	porph int	least altered	564468	644731	45.69	3.93	16.6	11.48	0.46	5.68	4.75	4.52	1.73	0.78
2531-1-887	Knockroe	porph int	least altered	564468	644731	45.75	2.6	16.06	17.34	0.28	3.38	3.38	5.58	1.66	1.24
2531-1-901	Knockroe	hyp. Int/flow	least altered	564468	644731	47.72	2.61	16.12	12.88	0.23	2.99	7.43	3.84	1.94	1.25
2638-28-100	Knockroe?	Tuff	mod chl-clay	563761	647587	39.12	3.72	12.02	13.18	0.12	12.7	6.07	0.23	1.64	0.68
2638-28-454	Knockroe	Diatreme	str chl-carb	563761	647587	43.12	4.13	13.26	10.18	0.09	2.84	8.96	0.58	3.69	0.78
2529-491-166	Knockseefin	Tuff	mod hem	564426	647255	38.89	2.9	13.91	12.27	0.27	6.98	9.97	1.93	1.54	0.62
2529-491-297	Knockroe	Tuff	wk-mod hem	564426	647255	55.1	1.46	16.64	8.4	0.1	1.4	3.04	4	5.37	0.28
2529-491-656	Knockroe	Tuff	mod chl	564426	647255	45.01	2.82	11.84	13.54	0.07	10.45	4.21	1.51	1.3	0.77
2564-1-108	Knockroe	hyp. Int/flow	least altered	579054	631849	43.8	3.21	14.65	14.14	0.17	6.86	9.59	2.24	1.58	0.52
2564-1-123	Knockroe	porph int	least altered	579054	631849	44	2.71	13.06	13.61	0.17	10.35	10	1.72	0.86	0.34
2564-1-128	Knockroe	porph int	least altered	579054	631849	44.21	2.67	12.91	13.64	0.19	9.93	10.15	1.83	0.89	0.33

Sample	LOI	Total	Li	C	S	Sc	V	Cr	Co	Ni	Cu	Zn	Ga	Ge	As	Se	Rb	Sr	Y	Zr	Nb	Mo	Ag
	%	%	ppm	%	%	ppm	ppm	ppm	ppm	ppm	ppm	ppm	ppm	ppm	ppm	ppm	ppm	ppm	ppm	ppm	ppm	ppm	ppm
2531-1-487	3.61	100.1	40	0.47	0.01	4.8	238	180	46	145	53	117	21.5	bdl	0.4	bdl	23.9	1030	28.9	308	77.9	2	bdl
2531-1-528	2.89	99.39	80	0.01	bdl	4.9	346	350	57	218	54	122	22.2	bdl	0.4	0.2	10.4	937	26.5	281	74.3	2	bdl
2531-1-545	3.3	99.92	50	0.02	bdl	5.4	332	320	55	212	58	117	21.4	bdl	0.4	0.4	12.4	949	27.3	288	76.7	1	bdl
2531-1-715	2.85	99.93	40	0.05	0.01	2	183	10	40	28	39	146	24	bdl	2	bdl	54.8	1195	30.8	438	95.9	4	bdl
2531-1-732	2.03	99.97	30	0.08	bdl	4.3	267	380	52	179	73	131	22.2	bdl	0.8	bdl	29	540	27.3	229	45.8	1	bdl
2531-1-748	2.97	99.89	50	0.03	0.01	4.5	241	300	53	164	68	121	21.6	bdl	1.5	0.2	20.2	451	26.3	220	43.1	1	bdl
2531-1-779	3	100.1	50	bdl	0.01	8.2	196	100	69	66	99	235	26.8	bdl	1	bdl	28.1	849	34	321	65.7	bdl	bdl
2531-1-792	3.41	99.87	50	0.02	bdl	10.2	201	80	42	51	23	199	28.3	bdl	0.9	0.2	20.5	716	35.1	317	64.9	bdl	bdl
2531-1-833	3.6	99.72	60	0.15	bdl	10.9	216	50	59	42	48	400	27.4	bdl	1.4	0.3	25.2	1120	31.9	304	64	1	bdl
2531-1-887	2.7	100.2	40	0.1	bdl	5.8	101	bdl	27	8	11	209	29.6	bdl	2.1	bdl	28.3	360	39.5	333	73.8	1	bdl
2531-1-901	2.66	100	40	0.28	0.02	4.5	89	bdl	25	8	15	143	22.8	bdl	3.2	bdl	33.7	871	39.5	330	72.6	3	bdl
2638-28-100	9.63	99.59	130	1.15	0.11	15.8	238	230	48	187	38	133	22.8	bdl	1.4	0.3	18.4	266	29.7	354	69.2	2	0.5
2638-28-454	11.57	99.89	50	2.54	0.17	13.7	271	310	38	205	18	34	26.6	bdl	2.5	bdl	121	136.5	31.4	409	74.8	1	0.6
2529-491-166	9.7	99.69	50	1.89	0.17	14.7	211	160	30	101	26	128	24	bdl	1.6	0.3	17.8	451	31.1	280	58.9	1	0.6
2529-491-297	3.57	99.69	10	0.58	bdl	3.1	71	20	10	10	4	154	38.6	bdl	1.4	bdl	116.5	434	64.8	975	177	2	0.5
2529-491-656	7.51	99.44	60	0.74	0.08	9.7	162	80	44	95	25	141	24.2	bdl	1.1	bdl	18	260	34.5	485	89.8	1	0.6
2564-1-108	3	100.05	50	0.26	0.01	6.6	301	150	49	93	85	128	21.6	bdl	0.4	bdl	30.4	606	26.8	249	54.1	1	bdl
2564-1-123	2.97	100.1	110	0.08	bdl	3.4	341	440	60	180	33	102	19	bdl	0.3	bdl	17.9	423	20	167	31.9	bdl	bdl
2564-1-128	2.6	99.68	70	0.09	bdl	3.6	307	400	58	172	26	102	17.7	bdl	0.4	bdl	20.6	416	19.1	162	30.8	1	bdl

Sample	Cd	In	Sn	Sb	Te	Cs	Ba	La	Ce	Pr	Nd	Sm	Eu	Gd	Tb	Dy	Ho	Er	Tm	Yb	Lu	Hf	Ta
	ppm	ppm	ppm	ppm	ppm	ppm	ppm	ppm	ppm	ppm	ppm	ppm	ppm	ppm	ppm	ppm	ppm	ppm	ppm	ppm	ppm	ppm	ppm
2531-1-487	0.8	0.035	3	bdl	0.01	2.03	863	49.4	97.3	11.3	44.8	8.92	2.78	8.08	1.1	5.86	1.1	2.63	0.37	2	0.3	6.8	3
2531-1-528	0.9	0.03	3	bdl	bdl	2.83	815	44.3	89.9	10.8	43.3	9.51	2.78	8.24	1.09	5.87	1.03	2.42	0.31	1.64	0.24	6.3	3.6
2531-1-545	0.9	0.032	3	bdl	bdl	1.05	846	45.4	92.4	11.2	44.4	9.58	2.91	8.37	1.09	5.65	1	2.44	0.33	1.63	0.25	6.3	3.9
2531-1-715	0.8	0.031	4	0.09	bdl	2.4	878	64.1	130	15.35	59.8	12.4	3.57	10.15	1.27	6.8	1.12	2.61	0.33	1.76	0.23	9.1	3.9
2531-1-732	0.7	0.042	2	bdl	bdl	0.61	358	34	70.9	8.64	34.5	7.52	2.14	6.97	0.95	5.37	1.01	2.55	0.37	2.03	0.34	5.4	2.1
2531-1-748	0.7	0.041	2	bdl	bdl	0.84	320	32.8	69.4	8.47	33.3	7.4	2.14	6.82	0.94	5.23	0.97	2.43	0.34	1.92	0.3	5.1	1.6
2531-1-779	bdl	0.073	3	0.05	bdl	1.24	301	48.3	104.5	13.1	53.8	11.9	3.32	10.15	1.31	6.98	1.3	2.97	0.41	2.26	0.33	7.2	3.4
2531-1-792	0.5	0.092	3	0.06	0.01	0.72	1300	47.4	104	13	53.8	11.9	3.28	10.45	1.36	7.18	1.31	3.18	0.44	2.3	0.32	7.1	2.4
2531-1-833	0.8	0.074	3	0.09	bdl	0.88	951	43.7	96.1	12.15	49.9	10.9	3.29	9.8	1.27	6.64	1.2	2.93	0.39	2.14	0.31	6.8	2.7
2531-1-887	0.7	0.053	3	0.06	bdl	0.56	359	57.8	122	15.05	61.8	12.95	4.14	11.6	1.52	7.83	1.51	3.63	0.5	2.63	0.4	7.4	2.8
2531-1-901	0.8	0.084	3	0.06	bdl	0.43	722	55.1	119.5	15.2	62.4	13.5	4.24	12	1.52	8.31	1.46	3.56	0.48	2.63	0.39	7.2	3.1
2638-28-100	0.5	0.08	2	0.06	bdl	2.57	512	42.4	90.4	11.75	50.1	11.3	3.07	9.23	1.19	6.48	1.07	2.68	0.36	2.08	0.33	8.7	3.8
2638-28-454	0.5	0.043	3	0.06	0.01	14.1	241	48.2	102	13.2	57	11.3	3.32	9.57	1.3	7.12	1.26	3.09	0.35	2.34	0.35	9.6	3.1
2529-491-166	0.5	0.077	3	bdl	bdl	1.07	325	43.3	87.6	10.85	46.8	9.18	3	8.62	1.2	6.46	1.16	2.94	0.37	2.43	0.33	7.3	1.4
2529-491-297	0.5	0.078	8	0.13	bdl	2.88	995	117	220	25.3	97.8	17.7	2.62	14.75	2.33	13	2.32	6.61	0.9	5.79	0.84	22.7	10.4
2529-491-656	0.5	0.09	3	0.06	0.01	1.92	215	63.4	126.5	15.15	61.9	11.25	3.26	9.69	1.22	7	1.25	3.3	0.44	2.52	0.39	11	3.9
2564-1-108	0.8	0.046	2	bdl	bdl	1.16	456	34.9	73.1	8.92	36.8	8.02	2.34	7.15	0.99	5.31	0.99	2.56	0.35	2.01	0.29	5.8	2.4
2564-1-123	0.9	0.024	2	bdl	0.01	4.17	242	21.9	46.5	5.78	23.9	5.74	1.71	5.3	0.75	4.21	0.8	1.87	0.26	1.44	0.2	4.1	1.3
2564-1-128	0.8	0.022	1	bdl	bdl	7.31	301	19.7	43	5.47	23.7	5.2	1.73	5.19	0.71	4.08	0.77	1.94	0.27	1.42	0.21	4.1	1.3

Sample	W	Re	Hg	Tl	Pb	Bi	Th	U
	ppm	ppm	ppm	ppm	ppm	ppm	ppm	ppm
2531-1-487	1	0.001	0.005	0.03	5	0.02	5.87	1.57
2531-1-528	2	bdl	0.007	bdl	3	0.01	5.12	1.33
2531-1-545	2	bdl	0.007	bdl	8	0.01	5.18	1.38
2531-1-715	2	bdl	0.007	0.05	4	0.02	7.16	1.87
2531-1-732	1	0.001	0.008	bdl	5	0.01	4.21	1.02
2531-1-748	1	0.001	0.01	0.03	5	0.01	4.12	0.97
2531-1-779	2	bdl	0.009	bdl	6	0.03	4.7	1.2
2531-1-792	2	bdl	0.006	bdl	6	0.02	4.86	1.45
2531-1-833	2	0.001	0.008	bdl	8	0.02	4.43	1.58
2531-1-887	2	0.001	0.009	bdl	bdl	0.02	5.57	1.49
2531-1-901	2	0.001	0.013	bdl	6	0.02	5.65	1.39
2638-28-100	1	0.001	0.012	0.02	3	0.02	5.22	1.41
2638-28-454	1	bdl	bdl	1.05	12	0.02	6.07	1.48
2529-491-166	1	0.001	0.005	0.03	2	0.02	5.04	1.38
2529-491-297	2	bdl	bdl	0.05	14	0.07	19.9	2.35
2529-491-656	1	0.001	bdl	0.05	7	0.03	7.84	2.16
2564-1-108	1	0.001	0.008	bdl	5	0.02	3.94	1.07
2564-1-123	2	bdl	0.007	bdl	4	0.01	2.39	0.69
2564-1-128	1	bdl	0.012	bdl	2	0.02	2.36	0.65